Open access • Journal Article • DOI:10.1107/S205322961900144X

The structure of the anti-aging agent J147 used for treating Alzheimer's disease

Guy J. Clarkson, M. Ángeles Farrán, Rosa M. Claramunt, Ibon Alkorta ...+1 more authors

Institutions: University of Warwick, National University of Distance Education, Spanish National Research Council

Published on: 01 Mar 2019 - Acta Crystallographica Section C-crystal Structure Communications (International Union of Crystallography (IUCr))

STRUCTURAL CHEMISTRY

ISSN 2053-2296

The structure of the anti-aging agent J147 used for treating Alzheimer's disease

Guy J. Clarkson,[a] M. Ángeles Farrán,[b]* Rosa M. Claramunt,[b]* Ibon Alkorta[c] and José Elguero[c]

[a]Department of Chemistry, University of Warwick, Coventry CV4 7AL, England, [b]Departamento de Química Orgánica y Bio-Orgánica, Facultad de Ciencias, Universidad Nacional de Educación a Distancia, Senda del Rey 9, E-28040 Madrid, Spain, and [c]Instituto de Química Médica, Centro de Química Orgánica Manuel Lora-Tamayo, CSIC, Juan de la Cierva 3, E-28006 Madrid, Spain. *Correspondence e-mail: afarran@ccia.uned.es, rclaramunt@ccia.uned.es

Received 12 December 2018
Accepted 25 January 2019

Edited by D. S. Yufit, University of Durham, England

Keywords: J147; DFT calculations; NMR; crystal structure; Alzheimer's disease; GIAO calculations; anti-aging agent.

CCDC reference: 1869097

Supporting information: this article has supporting information at journals.iucr.org/c

The molecular structure of the anti-aging agent **J147** [systematic name: (*E*)-*N*-(2,4-dimethylphenyl)-2,2,2-trifluoro-*N*′-(3-methoxybenzylidene)acetohydrazide], $C_{18}H_{17}F_3N_2O_2$, has been determined at 150 K. The crystal structure corresponds to the minimum-energy conformation in the gas phase calculated by density functional theory (DFT). 15 other conformations have been calculated and compared with the minimum, denoted **1111**. NMR spectroscopic data have been obtained and compared with those from Gauge Independent Atomic Orbital (GIAO) calculations. DFT calculations allow the reduction of the 16 possible rotamers to the four most stable (*i.e.* **1111**, **1112**, **1121** and **1222**); in addition, the calculated barriers connecting these minima are low enough to permit their interconversion. Comparison of the NMR spectroscopic results, both experimental and calculated, point to the **1121** isomer being present in chloroform solution.

1. Introduction

In a recent publication (Farrán *et al.*, 2018*b*), we used the structure of **J147** to design a series of 5-CF_3-1*H*-triazoles that were afterwards tested as neuroprotective agents (Farrán *et al.*, 2018*a*). The crystal structure of **J147** has been reported previously, however, it has not yet been deposited in the Cambridge Structural Database (CSD, Version 5.39, updated August 2018; Groom *et al.*, 2016; checked on September 21, 2018). To the best of our knowledge, the only information on the solid-state structure of **J147** is the low-quality black-and-white picture shown in Fig. 1 (Chen *et al.*, 2011).

To gain further insight into the conformational preferences of **J147**, one of the most promising molecules both for treating Alzheimer's disease and for preventing neurological problems associated with aging (Prior *et al.*, 2014; Daugherty *et al.*, 2017, 2018; Goldberg *et al.*, 2018), we carried out a computational analysis, a solution NMR spectroscopic study and determined the solid-state crystal structure.

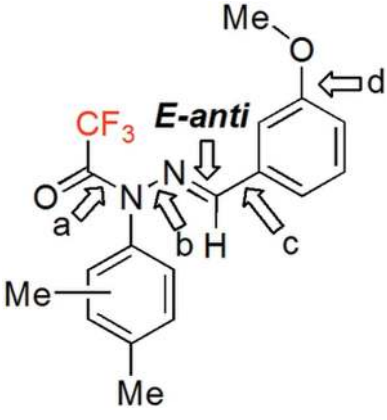

2. Experimental

2.1. Synthesis

J147 was prepared in two steps using a procedure modified from Wang *et al.* (2013), as depicted in Scheme 1.

2.1.1. Preparation of 1-(2,4-dimethylphenyl)-2-(3-methoxybenzylidene)hydrazine, 1. (2,4-Dimethylphenyl)hydrazine hydrochloride (951 mg, 5.51 mmol) was added to a solution of sodium acetate (452 mg, 5.51 mmol) in water (5 ml). A solution of 3-methoxybenzaldehyde (500 mg, 3.67 mmol) in EtOH

(3 ml) was then added slowly over a period of 5 min. The reaction mixture was heated to 100 °C and kept stirring for an additional 20 min until the disappearance of the starting materials monitored by thin-layer chromatography. The mixture was then cooled to 0 °C in an ice bath and a sticky orange oil precipitated. The remaining liquid fraction was decanted from the residue and washed with cold water. After drying under vacuum, the residue was used in the next step without further purification.

^{1}H NMR (400 MHz, $CDCl_3$): δ 7.74 (1H, *s*, H-3′), 7.45 (1H, *d*, ^3J = 8.2 Hz, H-5′), 7.31–7.25 [2H, *m*, H-5″, H-6 (C═N)], 7.20 (1H, *dt*, ^3J = 7.8, ^4J = 1.3 Hz, H-4″), 7.03 (1H, *dd*, ^3J = 8.2, 2.1 Hz, H-6′), 6.93–6.91 (1H, *m*, H-2″), 6.86 (1H, *ddd*, *J* = 8.1, 2.7, 1.1 Hz, H-6″), 3.87 (3H, *s*, OCH_3, H-15), 2.29 (3H, *s*, CH_3, H-12), 2.22 (3H, *s*, CH_3, H-10). ^{13}C NMR (101 MHz, $CDCl_3$): δ 159.8 (C-3″), 140.2 (C-4′), 137.5 (C-3′), 136.9 (C-1″), 131.1 (C-2′), 129.5 (C6, C═N)], 129.2 (C-2′), 127.7 (C-6′), 120.4 (C-1′), 119.2 (C-4″), 114.5 (C-6″), 113.2 (C-3′), 110.5 (C-5″), 55.3 (C-14, OMe), 20.5 (C-10), 17.0 (C-9).

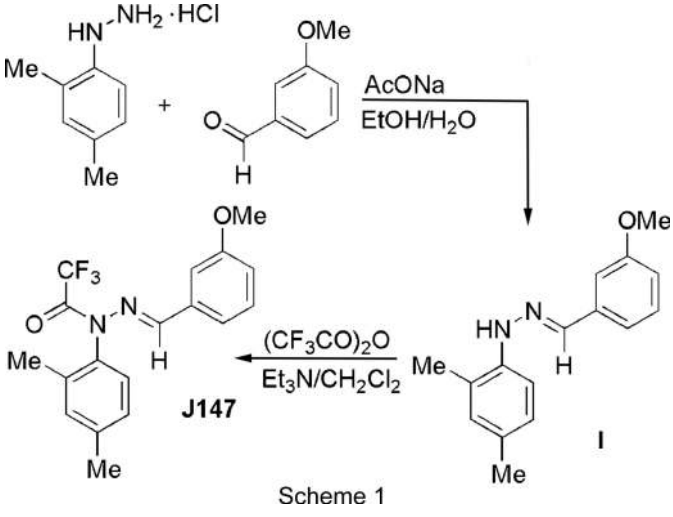

Scheme 1

2.1.2. (*E*)-*N*-(2,4-Dimethylphenyl)-2,2,2-trifluoro-*N*′-(3-methoxybenzylidene)acetohydrazide, J147. A solution of 1-(2,4-dimethylphenyl)-2-(3-methoxybenzylidene)hydrazine (500 mg, 1.97 mmol) and Et_3N (0.33 ml, 2.36 mmol) in CH_2Cl_2 (5 ml) was placed in a round-bottomed flask and cooled to 0 °C in an ice bath, after which trifluoroacetic anhydride (0.33 ml, 2.36 mmol) was added dropwise under a nitrogen atmosphere. The reaction mixture was stirred at this temperature for 1.5 h. After the mixture had been concentrated under vacuum, the residue was purified by column

Table 1
Experimental details.

Crystal data	
Chemical formula	$C_{18}H_{17}F_3N_2O_2$
M_r	350.33
Crystal system, space group	Monoclinic, $P2_1/c$
Temperature (K)	150
a, *b*, *c* (Å)	15.0494 (3), 14.2369 (3), 7.9898 (2)
β (°)	99.025 (2)
V (Å^3)	1690.68 (7)
Z	4
Radiation type	Cu $K\alpha$
μ (mm^{-1})	0.97
Crystal size (mm)	0.2 × 0.08 × 0.02
Data collection	
Diffractometer	Rigaku Oxford Diffraction SuperNova diffractometer with a dual source (Cu at zero) equipped with an AtlasS2 CCD area detector
Absorption correction	Multi-scan (*CrysAlis PRO*; Rigaku OD, 2018)
T_{min}, T_{max}	0.792, 1.000
No. of measured, independent and observed [$I > 2\sigma(I)$] reflections	5945, 5945, 4685
R_{int}	0.037 (for all HKLF5 reflections)
(sin $\theta/\lambda)_{max}$ (Å^{-1})	0.622
Refinement	
$R[F^2 > 2\sigma(F^2)]$, $wR(F^2)$, S	0.035, 0.096, 0.99
No. of reflections	5945
No. of parameters	230
H-atom treatment	H-atom parameters constrained
$\Delta\rho_{max}$, $\Delta\rho_{min}$ (e Å^{-3})	0.21, −0.23

Computer programs: *CrysAlis PRO* (Rigaku OD, 2018), *SHELXT* (Sheldrick, 2015*a*), *SHELXL2018* (Sheldrick, 2015*b*) and *OLEX2* (Dolomanov *et al.*, 2009).

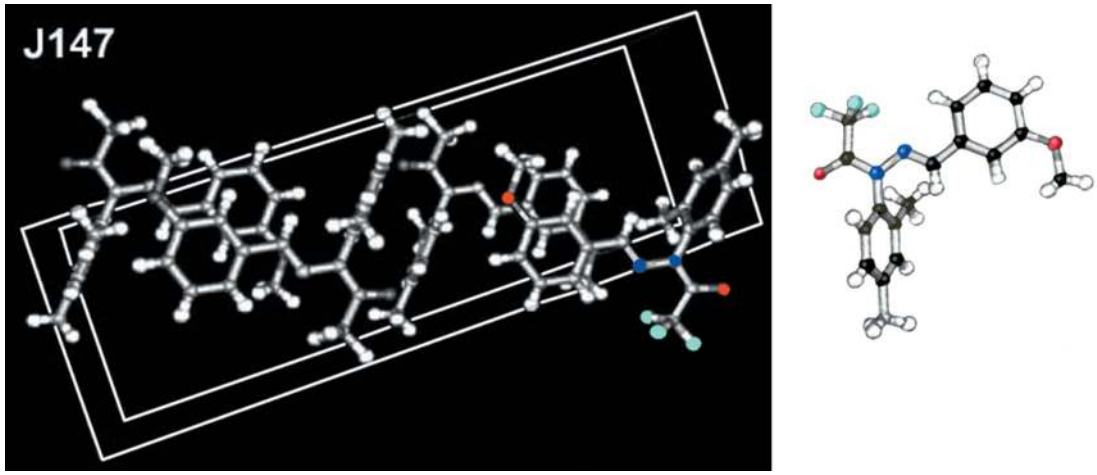

Figure 1
(Left) Picture taken from Chen *et al.* (2011) illustrating their crystal structure determination of **J147**. (Right) An individual molecule of **J147** (Farrán *et al.*, 2018*b*). The colours have been added by the present authors.

chromatography using a mixture of acetone/hexanes (1:10 *v*/*v*) as eluent to afford **J147** (yield 571 mg, 83%) as a pale-pink oil. A second column was needed to remove slight impurities and the compound was then recrystallized from ethanol/water at −4 °C. White crystals suitable for single-crystal X-ray diffraction analysis were obtained.

^{1}H NMR (400 MHz, $CDCl_3$): δ 7.29 (1H, *d*, ^3J = 7.9 Hz, H-5″), 7.27–7.23 [3H, *m*, H-2″, H-3′, H-6 (C═N)], 7.21 (1H, *d*, *J* = 7.9 Hz, H-5′), 7.12 (1H, *d*, ^3J = 7.2 Hz, H-4″), 7.05 (1H, *d*, ^3J = 7.9 Hz, H-6′), 6.95 (*ddd*, *J* = 8.3, 2.6, 1.0 Hz, 1H, H-6″), 3.83 (*s*, 3H, OCH_3, H-15), 2.42 (*s*, 3H, CH_3, H-12), 2.09 (*s*, 3H, CH_3, H-10). ^{13}C NMR (101 MHz, $CDCl_3$): δ 159.9 (C-3″), 157.3 (*d*, $\underline{C}OCF_3$, ^3J_F = 36 Hz), 143.9 (C6, C═N), 140.9 (C-4′), 136.2 (C-2′), 134.7 (C-1″), 132.6 (C-3′), 129.8 (C-5″), 129.6 (C-1′), 128.7 (C-5′), 128.5 (C-6′), 121.2 (C-1″), 117.1 (C-6″), 117.2 [*q*, ($CO\underline{C}F_3$) ^2J_F = 287 Hz], 111.7 (C-2″), 55.3 (C-14, OMe), 21.3 (C-10), 17.0 (C-9). ^{19}F (379.5 MHz, $CDCl_3$): δ −69.5.

2.2. Crystallography

Crystal data, data collection and structure refinement details are summarized in Table 1. Single crystals of **J147** were grown from water–ethanol. A crystal suitable for X-ray structure analysis was selected and mounted on a glass fiber with Fomblin oil.

The harvesting of the spots and integration was performed with the twin module in the *CrysAlis PRO* software package (Agilent, 2014). The twin ratio refined to 75:25 with the twin components related by a 180° rotation around the vector (100) in direct space. H atoms were given isotropic displacement parameter equal to 1.2 (or 1.5 for methyl H atoms) times the equivalent isotropic displacement parameter of the C atom to which they are attached.

2.3. NMR experiments

NMR spectra were recorded on a Bruker DRX 400 (9.4 Tesla, 400.13 MHz for ^{1}H, 100.61 MHz for ^{13}C and 40.54 MHz for ^{15}N), using a 5 mm inverse-detection H-X probe equipped with a z-gradient coil, at 300 K. Chemical shifts (δ in ppm) are given from the internal solvent; $CDCl_3$ =7.26 and 77.0 for ^{1}H and ^{13}C, respectively, were used as external references. Signals were characterized as *s* (singlet), *d* (doublet), *t* (triplet), *q* (quartet) and *m* (multiplet), and *J* couplings are given in Hz.

Typical parameters for ^{1}H NMR spectra were a spectral width of 4800 Hz and a pulse width of 9.5 ms at an attenuation level of 0 dB. Typical parameters for ^{13}C NMR spectra were a spectral width of 21 kHz, a pulse width of 12.5 ms at an attenuation level of −6 dB and a relaxation delay of 2 s. WALTZ-16 was used for broadband proton decoupling; the FIDS (free induction decays) were multiplied by an exponential weighting (lb = 1 Hz) before Fourier transformation.

Inverse proton-detected heteronuclear shift correlation spectra, (^{1}H–^{13}C) gs-HMQC and (^{1}H–^{13}C) gs-HMBC, were acquired and processed using standard Bruker NMR software in nonphase-sensitive mode. Gradient selection was achieved through a 5% sine truncated shaped pulse gradient of 1 ms.

Table 2
Calculated and experimental chemical shifts (δ, ppm) in $CDCl_3$ (note that the NMR atom numbering is different from the crystallographic atom numbering).

NMR atoms	X-ray atoms	**1111**	**1112**	**1121**	**1122**	Experimental
C1 (C═O)	C2	155.8	156.2	156.0	156.0	157.3 (*q*), ^2J_F = 36 Hz
C2 (CF_3)	C1	121.2	121.1	121.1	121.1	117.2 (*q*), ^1J_F = 287 Hz
C6 (C═N)	C5	141.2	140.8	141.1	141.1	143.9
H8 (C6—H)	H5	7.02	6.97	6.94	6.95	7.26 (under the solvent)
C1′	C12	132.1	132.2	132.6	132.4	129.6
C2′	C13	140.1	140.1	140.4	140.2	136.2
C3′	C14	131.5	131.6	131.6	131.7	132.6
C4′	C15	142.4	142.3	142.3	142.4	140.9
C5′	C16	127.6	127.6	127.5	127.6	128.7
C6′	C17	129.3	129.5	129.6	129.5	128.5
C1″	C6	136.1	136.2	135.8	136.4	134.7
C2″	C7	104.7	115.0	110.0	120.4	111.7
C3″	C8	161.4	160.7	160.4	160.4	159.9
C4″	C9	121.1	109.7	119.7	108.6	121.2
C5″	C10	128.6	128.7	129.8	129.7	129.8
C6″	C11	122.6	122.1	118.1	117.7	117.1
C9 (Me-2′)	C13*a*	17.9	17.9	17.9	17.9	17.0
H10 (Me-2′)	H13*a*	2.03	2.03	2.04	2.03	2.09
C11 (Me-4′)	C15*a*	21.2	21.2	21.2	21.2	21.3
H12 (Me-4′)	H15*a*	2.40	2.41	2.39	2.40	2.42
C14 (O—Me)	C18	53.0	52.6	52.2	52.5	55.2
H15 (O—Me)	H18	3.78	3.69	3.54	3.63	3.83
H3′	H14	7.21	7.20	7.24	7.22	7.24
H5′	H16	7.17	7.18	7.17	7.19	7.21
H6′	H17	6.96	6.97	6.98	6.98	7.03
H2″	H7	7.60	7.98	6.13	6.57	7.27
H4″	H9	6.99	6.56	6.96	6.51	7.12
H5″	H10	7.09	7.12	7.27	7.27	7.29
H6″	H11	6.52	6.49	7.99	7.93	6.95

Selected parameters for (^{1}H–^{13}C) gs-HMQC and (^{1}H–^{13}C) gs-HMBC spectra were a spectral width of 4800 Hz for ^{1}H and 20.5 kHz for ^{13}C, 1024 × 256 data set, number of scans = 2 (gs-HMQC) or 4 (gs-HMBC) and a relaxation delay of 1 s. The FIDs were processed using zero filling in the F1 domain and a sine-bell window function in both dimensions was applied prior to Fourier transformation. In the gs-HMQC experiments, GARP modulation of ^{13}C was used for decoupling.

^{19}F NMR spectra were recorded on the same spectrometer (376.50 MHz for ^{19}F), using a 5 mm QNP direct-detection probe head equipped with a z-gradient coil, at 300 K. Chemical shifts (δ in ppm) are given from $CFCl_3$ as external reference [one drop of $CFCl_3$ in 0.6 ml $CDCl_3$ (0.00)]. Typical parameters for ^{19}F NMR spectra were a spectral width of 55 kHz, a pulse width of 13.75 ms at an attenuation level of −6 dB and a relaxation delay of 1 s. WALTZ-16 was used for broadband proton decoupling; ^{19}F{^{1}H} and the FIDs were multiplied by an exponential weighting (lb = 1 Hz) before Fourier transformation.

2.4. Computational details

B3LYP/6-311++G(d,p) calculations (Ditchfield *et al.*, 1971; Frisch *et al.*, 1984) were carried out using *GAUSSIAN16* (Frisch *et al.*, 2016). Frequency calculations show that all the reported structures are minima (number of imaginary frequencies = 0). Theoretical calculations of the absolute shieldings (σ, ppm) and their transformation into chemical

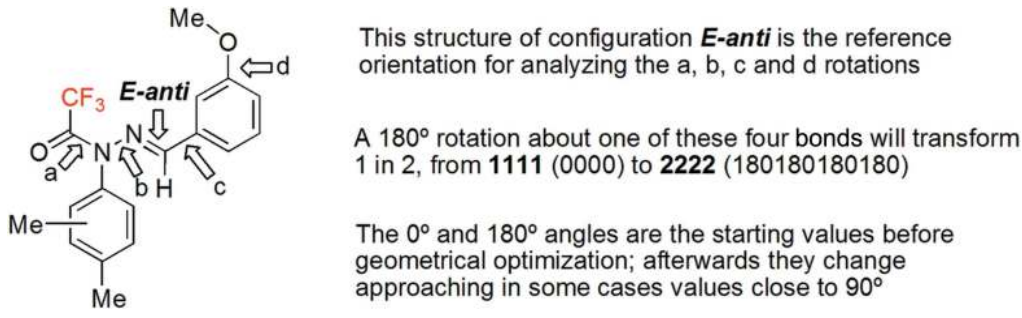

Figure 2
The structure of the reference starting orientation and the rotatable bond-numbering system.

shifts (δ, ppm) were carried out at the GIAO/B3LYP/6-311++G(d,p) level, as described in previous papers (Claramunt *et al.*, 2006; Blanco *et al.*, 2007; Infantes *et al.*, 2018).

3. Results and discussion

3.1. Theoretical exploration of the conformation of J147

The *E*/*Z* configuration about the C=N double bond requires high energies, about 150 kJ mol^{-1}, to isomerize (Blanco *et al.* 2009) it and is *E* in the illustration in Chen *et al.* (2011), corresponding to the most stable isomer according to calculations. Besides the hydrazone, there are four single bonds that can be rotated, *i.e.* **a**, **b**, **c** and **d**, leading to $2^4 = 16$ rotamers (Fig. 2). In the supporting information, the 16 possible rotamers are reported. Rotamer **1111** was selected as the reference compound because the calculations performed showed that it is the most stable of the 16 rotamers.

B3LYP/6-311++G(d,p) calculations show that the four most stable rotamers are those represented in Fig. 3. The remaining 12 rotamers have energy values ranging from 16 to 38 kJ mol^{-1} higher.

It appears that the previously reported structure corresponds to the **1121** rotamer with an energy 5.1 kJ mol^{-1} higher than for the **1111** rotamer. However, since the energy difference between these rotamers is relatively small, all of them must co-exist to varying degrees in solution. Four transition states (see supporting information) that connect the four minima were calculated in order to verify their low value and to prove that thermodynamic equilibrium should be reached instantly: $\mathbf{TS}_{\mathbf{1111–1112}} = 16.3$, $\mathbf{TS}_{\mathbf{1111–1121}} = 32.3$, $\mathbf{TS}_{\mathbf{1112–1122}} = 27.5$ and $\mathbf{TS}_{\mathbf{1121–1122}} = 11.8$ kJ mol^{-1} (see Fig. 4).

The 16 relative energies (kJ mol^{-1}) can be analyzed using a presence–absence matrix (0, angle = 0°; 1, angle 180°) that is **a**, **b**, **c** and **d** have the values 0 or 1 for the different **xxxx** conformers, for instance, **1221** = 0110. Preliminary tests show that these angles are related two-by-two, *i.e.* **a** with **b** and **c** with **d**, and adding two cross-terms (**a** − 1)(**b** − 1) and (**c** − 1)(**d** − 1), we obtain:

$E_{\rm rel}$ (kJ mol^{-1}) = (17.0±0.3)(**a** − 1) + (33.4±0.3)(**b** − 1) + (4.6±0.3)(**c** − 1) + (4.7±0.3)(**d** − 1) − (29.2±0.5)[(**a** − 1)(**b** − 1)] − (5.5±0.5)[(**c** − 1)(**d** − 1)], $n = 16$, $R^2 = 1.000$, r.m.s. = 0.6 kJ mol^{-1}.

Rotations about bonds **a** and **b** decreases the stability (increases the relative energy) by 17.0 and 33.4 kJ mol^{-1}, while rotations about the methoxyphenyl ring (**c** bond) and about the methoxy substituent (**d** bond) have lesser effects (4.6–4.7 kJ mol^{-1}). Of both cross-terms, clearly the rotations around bonds **a** and **b** are strongly related, which is apparent from an examination of the structures, where the proximity of the –CF_3 and C—H groups (structures **12xx**) is strongly disfavoured. Correlation between bonds **c** and **d** is much weaker (5.5 kJ mol^{-1}).

3.2. Determination of the X-ray structure of J147

Crystals were grown from an ethanol/water solution. All crystals examined exhibited twinning; the extent of twinning for each crystal investigated was estimated visually by checking the frames from the pre-experiment and examining the twinned spots. The strongest diffracting sample that appeared to have the least twinning was chosen and the data

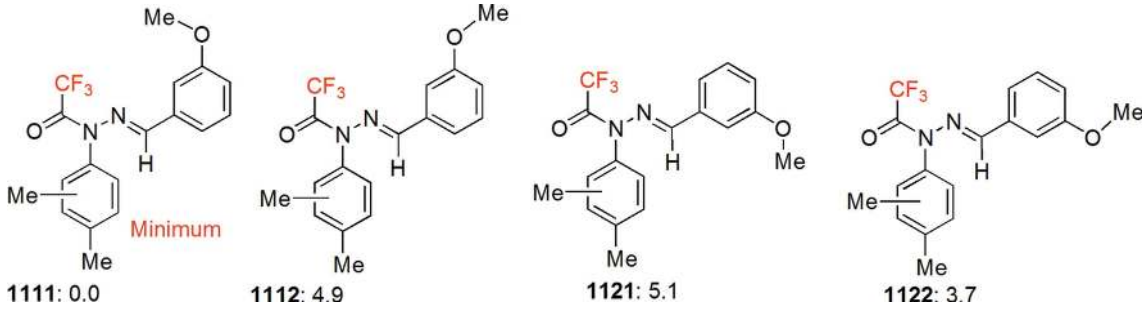

Figure 3
The four most stable predicted rotamers (energy values in kJ mol^{-1}).

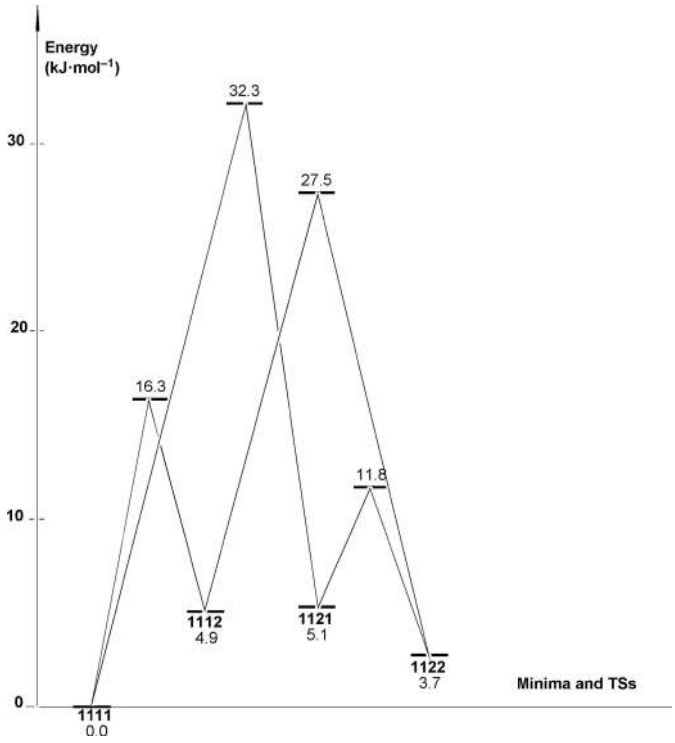

Figure 4
The four most stable minima and the four transition states connecting them.

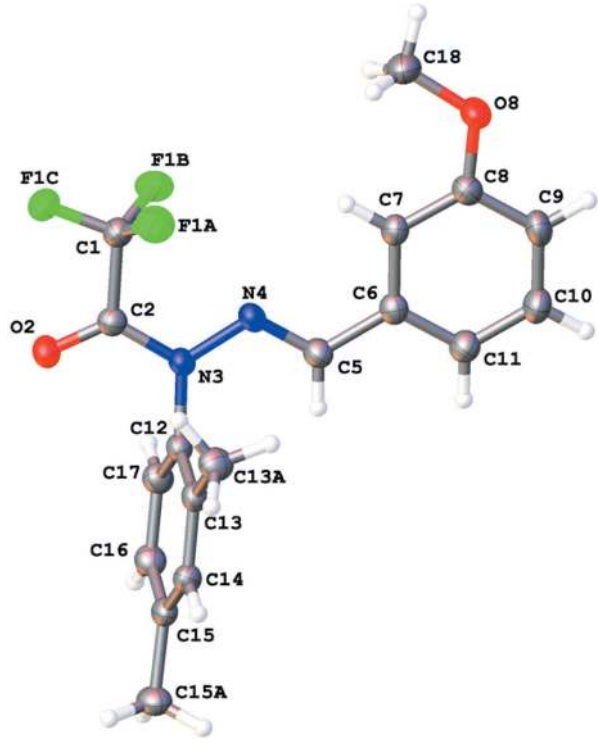

Figure 5
The X-ray structure of **J147** determined in this article, corresponding to the **1111** rotamer shown with crystallographic atom numbering.

were recorded for that sample. The asymmetric unit contains one molecule. The twin ratio refined to 75:25 and the two twin components are related by a rotation of 180.0° around the following vectors: reciprocal space (*hkl*) = 0.9591 −0.0004 −0.2832; direct space (*uvw*) = 1.0000 −0.0000 −0.0000. This orientation observed in the solid state corresponds to the minimum **1111** (Fig. 5).

There are no direction-specific interactions between the molecules in the solid state. **J147** contains no strong hydrogen-bond donors and relatively weak hydrogen-bond acceptors in the form of the F atoms and the trifluoroacetamide carbonyl [CF_3—C(═O)—N] group. The short contacts between the weak acceptors and the poor C—H donors of the aromatic rings and the methyl groups are > 2.6 Å or alternatively between the acceptor and donor atoms are > 3.4 Å, indicating no strong interactions. Though some of the aromatic rings are parallel, there is little or no overlap to indicate possible π-stacking interactions.

3.3. NMR characterization

The NMR data for **J147** in $CDCl_3$ have been reported previously (Chiruta *et al.*, 2013), but not assigned and with some signals not belonging to **J147**. In order to clarify this, we recorded the ^{1}H, ^{13}C and ^{19}F NMR spectra. Experimental chemical shifts, along with those calculated for different rotamers, are shown in Table 2.

The unassigned chemical shifts of **J147** in $CDCl_3$ (Chiruta *et al.* 2013) only partially coincide with those we have determined anew in the same solvent and with unambiguous assignments (Table 2). The linear regressions corresponding to the four isomers are:

Exp. = (0.2±0.7) + (0.995±0.007)*(**1111**), R^2 = 0.9987, r.m.s. error = 2.3 ppm
Exp. = (0.3±0.8) + (0.996±0.009)*(**1111**), R^2 = 0.9979, r.m.s. error = 2.9 ppm
Exp. = (0.2±0.5) + (0.996±0.005)*(**1121**), R^2 = 0.9993, r.m.s. error = 1.7 ppm
Exp. = (0.3±1.0) + (0.995±0.010)*(**1122**), R^2 = 0.9973, r.m.s. error = 3.3 ppm.

The **1121** isomer (the previously reported solid-state orientation) appears to be the best candidate for the structure of **J147** in chloroform solution.

4. Conclusions

The orientation depicted in Fig. 1 corresponds to the **1121** rotamer about bond **c** of the **1111** orientation of the structure determined in this article. In $CDCl_3$ solution, on the other hand, the **1121** rotamer appears to be predominant. Both results are of much interest for future studies of **J147** in the solid state (polymorphism) and in solution.

Acknowledgements

Computer, storage and other resources from the CTI (CSIC) are gratefully acknowledged.

Funding information

Funding for this research was provided by: Ministerio de Economía, Industria y Competitividad, Gobierno de España (grant Nos. CTQ2014-56833-R and CTQ2015-63997-C2-2-P); Comunidad Autónoma de Madrid (Spain) (grant No. S2013/MIT-2841, Fotocarbon).

References

Agilent (2014). *CrysAllis PRO*. Agilent Technologies Ltd, Yarnton, Oxfordshire, England.

Blanco, F., Alkorta, I. & Elguero, J. (2007). *Magn. Reson. Chem.* **45**, 797–800.

Blanco, F., Alkorta, I. & Elguero, J. (2009). *Croat. Chem. Acta*, **82**, 173–183.

Chen, Q., Prior, M., Dargusch, R., Roberts, A., Riek, R., Eichmann, C., Chiruta, C., Akaishi, T., Abe, K., Maher, P. & Schubert, D. (2011). *PLoS One*, **6**, e27865.

Chiruta, C., Zhao, Y., Tang, F., Wang, T. & Schubert, D. (2013). *Bioorg. Med. Chem.* **21**, 2733–2741.

Claramunt, R. M., Cornago, P., Torres, V., Pinilla, E., Torres, M. R., Samat, A., Lokshin, V., Valés, M. & Elguero, J. (2006). *J. Org. Chem.* **71**, 6881–6891.

Daugherty, D., Goldberg, J., Fischer, W., Dargush, R., Maher, P. A. & Schubert, D. (2017). *Alzheimers Res. Ther*. **9**, article No. 50.

Daugherty, D. J., Marquez, A., Calcutt, N. A. & Schubert, D. (2018). *Neuropharmacology*, **129**, 26–35.

Ditchfield, R., Hehre, W. J. & Pople, J. A. (1971). *J. Chem. Phys.* **54**, 724–728.

Dolomanov, O. V., Bourhis, L. J., Gildea, R. J., Howard, J. A. K. & Puschmann, H. (2009). *J. Appl. Cryst.* **42**, 339–341.

Farrán, M. A., Bonet, M. A., Claramunt, R. M., Moreno Fernández, C. A., Martínez Casanova, D. & Lavandera, J. L. (2018*a*). 18th Meeting of the 'Sociedad Española de Química Terapéutica', Salamanca, Spain, January 23–26, 2018.

Farrán, M. Á., Bonet, M. Á., Claramunt, R. M., Torralba, M. C., Alkorta, I. & Elguero, J. (2018*b*). *Acta Cryst.* C**74**, 513–522.

Frisch, M. J., Pople, J. A. & Binkley, J. S. (1984). *J. Chem. Phys.* **80**, 3265–3269.

Frisch, M. J. *et al.* (2016). *GAUSSIAN16*. Revision A.03. Gaussian Inc., Wallingford, CT, USA. http://www.gaussian.com

Goldberg, J., Currais, A., Prior, M., Fischer, W., Chiruta, C., Ratliff, E., Daugherty, D., Dargusch, R., Finley, K., Esparza-Moltó, P. B., Cuezva, J. M., Maher, P., Petrascheck, M. & Schubert, D. (2018). *Aging Cell*, **17**, e12715.

Groom, C. R., Bruno, I. J., Lightfoot, M. P. & Ward, S. C. (2016). *Acta Cryst.* B**72**, 171–179.

Infantes, L., Moreno, J. M., Claramunt, R. M., Sanz, D., Alkorta, I. & Elguero, J. (2018). *Inorg. Chim. Acta*, **483**, 402–410.

Prior, M., Chiruta, C., Currais, A., Goldberg, J., Ramsey, J., Dargusch, R., Maher, P. A. & Schubert, D. (2014). *ACS Chem. Neurosci.* **5**, 503–513.

Rigaku OD (2018). *CrysAlis PRO*. Rigaku Oxford Diffraction Ltd, Yarnton, Oxfordshire, England.

Sheldrick, G. M. (2015). *Acta Cryst.* A**71**, 3–8.

Wang, M., Gao, M. & Zheng, K. H. (2013). *Bioorg. Med. Chem. Lett.* **23**, 524–527.

supporting information

Acta Cryst. (2019). C**75**, 271-276 [https://doi.org/10.1107/S205322961900144X]

The structure of the anti-aging agent J147 used for treating Alzheimer's disease

Guy J. Clarkson, M. Ángeles Farrán, Rosa M. Claramunt, Ibon Alkorta and José Elguero

Computing details

Data collection: *CrysAlis PRO* (Rigaku OD, 2018); cell refinement: *CrysAlis PRO* (Rigaku OD, 2018); data reduction: *CrysAlis PRO* (Rigaku OD, 2018); program(s) used to solve structure: SHELXT (Sheldrick, 2015a); program(s) used to refine structure: *SHELXL2018* (Sheldrick, 2015b); molecular graphics: OLEX2 (Dolomanov *et al.*, 2009); software used to prepare material for publication: OLEX2 (Dolomanov *et al.*, 2009).

(*E*)-*N*-(2,4-Dimethylphenyl)-2,2,2-trifluoro-*N*′-(3-methoxybenzylidene)acetohydrazide

Crystal data

$C_{18}H_{17}F_3N_2O_2$
$M_r = 350.33$
Monoclinic, $P2_1/c$
$a = 15.0494$ (3) Å
$b = 14.2369$ (3) Å
$c = 7.9898$ (2) Å
$\beta = 99.025$ (2)°
$V = 1690.68$ (7) Å^3
$Z = 4$
$F(000) = 728$
$D_x = 1.376$ Mg m^{-3}
Cu $K\alpha$ radiation, $\lambda = 1.54184$ Å
Cell parameters from 8396 reflections
$\theta = 6.4$–$73.4°$
$\mu = 0.97$ mm^{-1}
$T = 150$ K
Block, colourless
0.2 × 0.08 × 0.02 mm

Data collection

Rigaku Oxford Diffraction SuperNova diffractometer with a dual source (Cu at zero) equipped with an AtlasS2 CCD area detector
Radiation source: micro-focus sealed X-ray tube, SuperNova (Cu) X-ray Source
Mirror monochromator
Detector resolution: 5.3046 pixels mm^{-1}
ω scans
Absorption correction: multi-scan (CrysAlis PRO; Rigaku OD, 2018)
$T_{min} = 0.792$, $T_{max} = 1.000$
5945 measured reflections
5945 independent reflections
4685 reflections with $I > 2\sigma(I)$
$R_{int} = 0.037$
$\theta_{max} = 73.5°$, $\theta_{min} = 3.0°$
$h = -18 \rightarrow 18$
$k = -17 \rightarrow 17$
$l = -9 \rightarrow 9$

Refinement

Refinement on F^2
Least-squares matrix: full
$R[F^2 > 2\sigma(F^2)] = 0.035$
$wR(F^2) = 0.096$
$S = 0.99$
5945 reflections
230 parameters
0 restraints
Primary atom site location: iterative
Hydrogen site location: inferred from neighbouring sites
H-atom parameters constrained
$w = 1/[\sigma^2(F_o^2) + (0.0644P)^2]$ where $P = (F_o^2 + 2F_c^2)/3$
$(\Delta/\sigma)_{max} < 0.001$
$\Delta\rho_{max} = 0.21$ e Å^{-3}
$\Delta\rho_{min} = -0.23$ e Å^{-3}

Special details

Geometry. All esds (except the esd in the dihedral angle between two l.s. planes) are estimated using the full covariance matrix. The cell esds are taken into account individually in the estimation of esds in distances, angles and torsion angles; correlations between esds in cell parameters are only used when they are defined by crystal symmetry. An approximate (isotropic) treatment of cell esds is used for estimating esds involving l.s. planes.

Refinement. Refined as a 2-component twin.
The twin ratio is 75:25. The twin components are related by a rotation = 179.9993 deg around the following vectors:
Reciprocal space (hkl): 0.9591 -0.0004 -0.2832 Direct space (uvw) : 1.0000 -0.0000 -0.0000
More twin information from Crysalis Pro is shown below HKLF 5 merged
RINT ANALYSIS FOR ALL HKLF5 REFLECTIONS Components measured unique redundancy F2/sig(F2) Rint Rsigma ——— 1,2 40817 6202 6.58 13.10 0.037 0.049
RINT ANALYSIS FOR OVERLAPPED REFLECTIONS Components measured unique redundancy F2/sig(F2) Rint Rsigma ——— 1,2 15535 2329 6.67 16.27 0.034 0.042
RINT ANALYSIS FOR ISOLATED REFLECTIONS Component measured unique redundancy F2/sig(F2) Rint Rsigma ——— 1 12639 1940 6.51 15.24 0.035 0.042 2 12643 1933 6.54 7.05 0.061 0.103

Fractional atomic coordinates and isotropic or equivalent isotropic displacement parameters (Å²)

	x	*y*	*z*	U_{iso}*/U_{eq}
C1	0.79743 (10)	0.55247 (11)	0.5015 (2)	0.0310 (3)
F1A	0.80312 (7)	0.52484 (8)	0.66192 (12)	0.0429 (2)
F1B	0.86916 (6)	0.52092 (7)	0.44165 (14)	0.0426 (3)
F1C	0.80174 (6)	0.64552 (7)	0.50186 (15)	0.0465 (3)
C2	0.70649 (9)	0.52283 (11)	0.39492 (18)	0.0269 (3)
O2	0.65540 (7)	0.58383 (8)	0.33280 (15)	0.0346 (3)
N3	0.68799 (8)	0.42978 (9)	0.38228 (16)	0.0274 (3)
N4	0.75575 (8)	0.36869 (9)	0.45448 (16)	0.0275 (3)
C5	0.74210 (9)	0.28083 (11)	0.43262 (19)	0.0292 (3)
H5	0.687429	0.258876	0.368883	0.035*
C6	0.81146 (9)	0.21384 (10)	0.50661 (19)	0.0279 (3)
C7	0.88960 (10)	0.24511 (11)	0.61040 (18)	0.0291 (3)
H7	0.898622	0.310195	0.633233	0.035*
C8	0.95351 (10)	0.18023 (11)	0.6793 (2)	0.0325 (3)
O8	1.03238 (8)	0.20262 (9)	0.77993 (18)	0.0448 (3)
C9	0.94022 (11)	0.08438 (12)	0.6455 (2)	0.0369 (4)
H9	0.984103	0.040119	0.693868	0.044*
C10	0.86373 (11)	0.05411 (12)	0.5422 (2)	0.0371 (4)
H10	0.855136	−0.010989	0.519015	0.045*
C11	0.79887 (10)	0.11852 (11)	0.4717 (2)	0.0328 (3)
H11	0.746236	0.097521	0.399995	0.039*
C12	0.59850 (9)	0.40011 (10)	0.30719 (19)	0.0261 (3)
C13	0.53748 (9)	0.37550 (10)	0.41401 (19)	0.0268 (3)
C13A	0.56160 (11)	0.37566 (12)	0.6041 (2)	0.0350 (3)
H13A	0.600629	0.321894	0.640011	0.052*
H13B	0.506618	0.371151	0.655018	0.052*
H13C	0.593278	0.434026	0.640896	0.052*
C14	0.45046 (9)	0.35210 (11)	0.3373 (2)	0.0286 (3)
H14	0.407817	0.333806	0.407057	0.034*

C15	0.42381 (9)	0.35456 (10)	0.1622 (2)	0.0283 (3)
C15A	0.32796 (10)	0.33260 (12)	0.0862 (2)	0.0371 (4)
H15A	0.311125	0.271072	0.126430	0.056*
H15C	0.322498	0.331594	−0.037665	0.056*
H15B	0.287938	0.380841	0.120305	0.056*
C16	0.48731 (10)	0.37919 (11)	0.0605 (2)	0.0309 (3)
H16	0.470708	0.380628	−0.059150	0.037*
C17	0.57474 (10)	0.40166 (11)	0.1329 (2)	0.0303 (3)
H17	0.617961	0.417993	0.063091	0.036*
C18	1.05443 (11)	0.29985 (13)	0.7989 (3)	0.0445 (4)
H18A	1.052627	0.328445	0.686869	0.067*
H18B	1.114964	0.306629	0.863909	0.067*
H18C	1.010847	0.331309	0.859057	0.067*

Atomic displacement parameters (Å²)

	U^{11}	U^{22}	U^{33}	U^{12}	U^{13}	U^{23}
C1	0.0286 (7)	0.0266 (8)	0.0363 (8)	−0.0010 (6)	0.0004 (6)	0.0005 (6)
F1A	0.0474 (5)	0.0470 (6)	0.0305 (5)	−0.0026 (4)	−0.0060 (4)	0.0000 (4)
F1B	0.0270 (4)	0.0430 (6)	0.0587 (6)	−0.0025 (4)	0.0091 (4)	−0.0025 (5)
F1C	0.0396 (5)	0.0269 (5)	0.0667 (7)	−0.0045 (4)	−0.0115 (5)	−0.0011 (5)
C2	0.0259 (6)	0.0274 (7)	0.0269 (7)	−0.0006 (5)	0.0027 (5)	0.0003 (6)
O2	0.0336 (5)	0.0257 (6)	0.0411 (6)	0.0028 (4)	−0.0044 (5)	0.0037 (5)
N3	0.0234 (5)	0.0240 (6)	0.0326 (7)	0.0016 (4)	−0.0020 (5)	0.0027 (5)
N4	0.0237 (5)	0.0266 (7)	0.0311 (6)	0.0039 (5)	0.0005 (5)	0.0027 (5)
C5	0.0274 (6)	0.0283 (8)	0.0305 (8)	0.0017 (5)	0.0001 (5)	−0.0008 (6)
C6	0.0287 (7)	0.0263 (7)	0.0289 (7)	0.0024 (5)	0.0051 (5)	0.0002 (6)
C7	0.0292 (7)	0.0235 (8)	0.0345 (7)	0.0016 (5)	0.0042 (5)	−0.0001 (7)
C8	0.0272 (7)	0.0309 (8)	0.0382 (8)	0.0014 (6)	0.0016 (6)	0.0025 (6)
O8	0.0332 (6)	0.0319 (7)	0.0627 (9)	0.0019 (5)	−0.0129 (5)	0.0040 (6)
C9	0.0361 (8)	0.0273 (8)	0.0465 (10)	0.0080 (6)	0.0036 (7)	0.0063 (7)
C10	0.0409 (8)	0.0245 (8)	0.0449 (9)	0.0020 (6)	0.0035 (7)	0.0000 (7)
C11	0.0333 (7)	0.0284 (8)	0.0355 (8)	0.0001 (6)	0.0019 (6)	−0.0023 (6)
C12	0.0247 (6)	0.0218 (7)	0.0302 (8)	0.0017 (5)	−0.0006 (5)	0.0007 (5)
C13	0.0293 (7)	0.0218 (7)	0.0281 (7)	0.0025 (5)	0.0009 (5)	0.0017 (6)
C13A	0.0350 (7)	0.0391 (9)	0.0294 (8)	−0.0005 (6)	0.0005 (6)	0.0035 (7)
C14	0.0273 (6)	0.0249 (7)	0.0333 (8)	−0.0005 (5)	0.0037 (6)	0.0028 (6)
C15	0.0277 (7)	0.0209 (7)	0.0346 (8)	0.0015 (5)	−0.0003 (6)	−0.0014 (6)
C15A	0.0293 (7)	0.0371 (9)	0.0422 (9)	−0.0019 (6)	−0.0030 (6)	−0.0052 (7)
C16	0.0326 (7)	0.0314 (8)	0.0269 (7)	0.0011 (6)	−0.0010 (6)	−0.0005 (6)
C17	0.0296 (7)	0.0310 (8)	0.0300 (8)	0.0003 (6)	0.0036 (6)	0.0027 (6)
C18	0.0346 (8)	0.0351 (10)	0.0592 (12)	−0.0045 (7)	−0.0067 (8)	0.0017 (8)

Geometric parameters (Å, º)

C1—F1A	1.3303 (19)	C11—H11	0.9500
C1—F1B	1.3260 (18)	C12—C13	1.393 (2)
C1—F1C	1.3262 (18)	C12—C17	1.382 (2)

C1—C2	1.5527 (19)	C13—C13A	1.505 (2)
C2—O2	1.2133 (18)	C13—C14	1.396 (2)
C2—N3	1.354 (2)	C13A—H13A	0.9800
N3—N4	1.3944 (16)	C13A—H13B	0.9800
N3—C12	1.4487 (17)	C13A—H13C	0.9800
N4—C5	1.275 (2)	C14—H14	0.9500
C5—H5	0.9500	C14—C15	1.394 (2)
C5—C6	1.468 (2)	C15—C15A	1.5076 (19)
C6—C7	1.401 (2)	C15—C16	1.393 (2)
C6—C11	1.392 (2)	C15A—H15A	0.9800
C7—H7	0.9500	C15A—H15C	0.9800
C7—C8	1.384 (2)	C15A—H15B	0.9800
C8—O8	1.3629 (19)	C16—H16	0.9500
C8—C9	1.399 (2)	C16—C17	1.389 (2)
O8—C18	1.426 (2)	C17—H17	0.9500
C9—H9	0.9500	C18—H18A	0.9800
C9—C10	1.376 (2)	C18—H18B	0.9800
C10—H10	0.9500	C18—H18C	0.9800
C10—C11	1.393 (2)		

F1A—C1—C2	111.48 (12)	C17—C12—N3	119.30 (13)
F1B—C1—F1A	108.32 (12)	C17—C12—C13	122.00 (13)
F1B—C1—F1C	107.26 (12)	C12—C13—C13A	122.68 (13)
F1B—C1—C2	114.04 (13)	C12—C13—C14	117.01 (13)
F1C—C1—F1A	107.32 (13)	C14—C13—C13A	120.30 (14)
F1C—C1—C2	108.13 (12)	C13—C13A—H13A	109.5
O2—C2—C1	118.51 (13)	C13—C13A—H13B	109.5
O2—C2—N3	124.06 (13)	C13—C13A—H13C	109.5
N3—C2—C1	117.39 (12)	H13A—C13A—H13B	109.5
C2—N3—N4	116.80 (11)	H13A—C13A—H13C	109.5
C2—N3—C12	118.88 (11)	H13B—C13A—H13C	109.5
N4—N3—C12	124.16 (12)	C13—C14—H14	118.8
C5—N4—N3	117.62 (12)	C15—C14—C13	122.48 (13)
N4—C5—H5	120.2	C15—C14—H14	118.8
N4—C5—C6	119.54 (13)	C14—C15—C15A	120.39 (14)
C6—C5—H5	120.2	C16—C15—C14	118.42 (13)
C7—C6—C5	120.64 (13)	C16—C15—C15A	121.18 (14)
C11—C6—C5	119.12 (13)	C15—C15A—H15A	109.5
C11—C6—C7	120.24 (14)	C15—C15A—H15C	109.5
C6—C7—H7	120.3	C15—C15A—H15B	109.5
C8—C7—C6	119.33 (14)	H15A—C15A—H15C	109.5
C8—C7—H7	120.3	H15A—C15A—H15B	109.5
C7—C8—C9	120.31 (14)	H15C—C15A—H15B	109.5
O8—C8—C7	124.41 (15)	C15—C16—H16	119.8
O8—C8—C9	115.27 (14)	C17—C16—C15	120.46 (14)
C8—O8—C18	117.16 (13)	C17—C16—H16	119.8
C8—C9—H9	119.9	C12—C17—C16	119.62 (14)
C10—C9—C8	120.13 (14)	C12—C17—H17	120.2

C10—C9—H9	119.9	C16—C17—H17	120.2
C9—C10—H10	119.9	O8—C18—H18A	109.5
C9—C10—C11	120.25 (15)	O8—C18—H18B	109.5
C11—C10—H10	119.9	O8—C18—H18C	109.5
C6—C11—C10	119.74 (14)	H18A—C18—H18B	109.5
C6—C11—H11	120.1	H18A—C18—H18C	109.5
C10—C11—H11	120.1	H18B—C18—H18C	109.5
C13—C12—N3	118.62 (13)		